J. Fluid Mech. (1983), *vol.* 134, *pp.* 161–177
Printed in Great Britain

Effect of boundary absorption upon longitudinal dispersion in shear flows

By RONALD SMITH

Department of Applied Mathematics and Theoretical Physics, University of Cambridge, Silver Street, Cambridge CB3 9EW

(Received 2 September 1982 and in revised form 20 May 1983)

Boundary absorption causes a depletion of contaminant. Since the boundary tends to be the region of lowest velocity and of strongest shear, the remaining contaminant experiences on average an increased advection velocity, a reduced rate of shear dispersion, and a tendency to develop skewness towards the rear. Here it is shown how all these effects can be incorporated into a delay-diffusion description of the longitudinal dispersion process (Smith 1981). It is the accurate reproduction of the skewness that permits a delay-diffusion equation to become applicable at an earlier stage than the more conventional diffusion-equation models for longitudinal dispersion, and before there has been an undue loss of contaminant through the boundary.

1. Introduction

In studies of shear-flow dispersion it often suffices to know bulk one-dimensional quantities rather than the detailed three-dimensional concentration distribution. Conventionally, this has led to model equations for the cross-sectionally averaged concentration $\bar{c}(x,t)$ (Taylor 1953). It has long been recognized that when there is cross-stream transport, for example the vertical drift of heavy particles, there can be substantial concentration variations across the flow (Aris 1959). However, the final model equations for longitudinal dispersion have nevertheless been obtained from a direct cross-sectional average of the full equations (e.g. Sankarasubramanian & Gill 1973, equations (6), (7)).

De Gance & Johns (1978*a*, *b*) have shown that for a one-dimensional diffusion model of longitudinal dispersion there is a mathematically preferred transverse average in which the coefficients take the simplest form. The weight function $\psi_0(y,z)$ for this preferred average is the lowest mode for the decay of transverse concentration variations. Equivalently, $\psi_0(y,z)$ is the shape of the asymptotic concentration profile across the flow:

$$c \sim c_0(x,t)\,\psi_0(y,z) \quad \text{as} \quad t \to \infty. \tag{1.1}$$

Thus at large times after discharge the relative importance given to different parts of the flow varies as ψ_0^2. One factor arises as the weight function and the second factor comes through the concentration profile across the flow.

Recently, Lungu & Moffatt (1982) have also identified a mathematically preferred average $F_0(K,y,z)$ in the Fourier-transform plane. In the limit of small wavenumber ($K \to 0$) their preferred average becomes the same as the weighting $\psi_0(y,z)$ advocated by De Gance & Johns (1978*a*, *b*), and again leads to a diffusion approximation for the longitudinal dispersion.

Although a diffusion model is valid on a sufficiently large length- or timescale, the author (Smith 1981) has shown that a telegraph or delay-diffusion equation can accurately reproduce the non-Gaussian longitudinal concentration distributions observed at moderately large times (Elder 1959, figure 4; Gill & Ananthakrishnan 1967, figure 5; Jayaraj & Subramanian 1978, figure 4). Here the preferred average identified by De Gance & Johns (1978*a*, *b*) is used to extend the delay diffusion model to incorporate the effects of absorption at boundaries.

The physical origin of the skewness lies in the relative profiles of velocity and concentration across the flow. For example, when there is strong boundary absorption most of the contaminant will be in the faster-moving part of the flow well away from the boundary. Thus the small amount of contaminant near the boundary will tend to be left far behind as an extended tail (i.e. negative skewness). This effect is particularly noticeable for Poiseuille pipe flow (see §5), since in the absence of boundary absorption there is a forwards tail (Taylor 1953, figure 6; Gill & Anantha-krishnan 1967, figure 5).

2. Transverse-diffusion eigenmodes

We write the full equations for the three-dimensional concentration $c(x, y, z, t)$:

$$\partial_t c + u(y,z)\,\partial_x c - \kappa(y,z)\,\partial_x^2 c - \boldsymbol{\nabla}\cdot(\kappa\boldsymbol{\nabla}c) = q(x,y,z,t), \tag{2.1a}$$

with

$$\kappa \boldsymbol{n}\cdot\boldsymbol{\nabla}c + \beta(y,z)\,c = 0 \quad \text{on } \partial A. \tag{2.1b}$$

Here $u(y,z)$ is the longitudinal velocity, $\kappa(y,z)$ the diffusivity, $\boldsymbol{\nabla}$ the transverse gradient operator $(0, \partial_y, \partial_z)$, $q(x,y,z,t)$ the source strength, ∂A the boundary, $\boldsymbol{n}$ the outwards normal, and $\beta(y,z)$ a first-order reaction coefficient. The wall mechanism can be thought of as being catalytic reaction, deposition, transport across a semipermeable membrane, or heat conduction.

The eigenmodes $\psi_m(y,z)$ for the decay of concentration variations across the flow satisfy the equations

$$\boldsymbol{\nabla}\cdot(\kappa\boldsymbol{\nabla}\psi_m) + \lambda_m\psi_m = 0, \tag{2.2a}$$

with

$$\kappa\boldsymbol{n}\cdot\boldsymbol{\nabla}\psi_m + \beta\psi_m = 0 \quad \text{on } \partial A. \tag{2.2b}$$

The eigenvalues ψ_m are all real, and, without loss of generality, we can normalize the modes

$$\overline{\psi_m^2} = 1, \quad \overline{\psi_j\,\psi_m} = 0 \quad (j \neq m), \tag{2.3}$$

where the overbars denote cross-sectional average values. The lowest mode is of particular importance since it is the asymptotic profile for the concentration variations across the flow at large times after discharge, i.e. because of their larger eigenvalues the higher modes decay away much more rapidly.

In terms of the eigenmodes we represent the source strength q:

$$q(x,y,z,t) = q_0(x,t)\,\psi_0(y,z) + \sum_{m=1}^{\infty} q_m(x,t)\,\psi_m(y,z). \tag{2.4}$$

Also, for later use we define the velocity and diffusivity coefficients

$$u_{00} = \overline{u\psi_0^2}, \quad u_{m0} = \overline{u\psi_m\,\psi_0}, \quad u_{mj} = \overline{u\psi_m\,\psi_j}, \tag{2.5}$$

$$\kappa_{00} = \overline{\kappa\psi_0^2}, \quad \kappa_{m0} = \overline{\kappa\psi_m\,\psi_0}, \quad \kappa_{mj} = \overline{\kappa\psi_m\,\psi_j}. \tag{2.6}$$

The author (Smith 1981, equation (3.6)) has given an alternative formula for the velocity coefficients when Reynolds' analogy is applicable (i.e. when there is a constant ratio between the diffusivity κ and the viscosity ν). The generalization to encompass boundary absorption is

$$u_{mm} = U + \frac{1}{\lambda_m A}\int_A (u-U)\,\kappa(\nabla\psi_m)^2\,\mathrm{d}A + \frac{1}{\lambda_m A}\int_{\partial A}\left\{\tfrac{1}{2}(\psi_m^2-1)\,\kappa\frac{\partial u}{\partial n} + \beta U\psi_m^2\right\}\mathrm{d}s, \tag{2.7a}$$

$$u_{mn} = \frac{1}{(\lambda_n-\lambda_m)A}\int_A \kappa(\psi_m\,\nabla\psi_n - \psi_n\,\nabla\psi_m)\cdot\nabla u\,\mathrm{d}A, \tag{2.7b}$$

where A is the cross-sectional area, and U is any convenient reference velocity.

3. Longitudinal-dispersion equation

In order to exploit the advantages of the mathematically preferred average (De Gance & Johns 1978*a*, §3.2*c*), we choose the dependent variable to be the amplitude $c_0(x,t)$ of the lowest mode $\psi_0(y,z)$:

$$c_0(x,t) = \overline{c\psi_0}. \tag{3.1}$$

Thus in solving (2.1*a*, *b*) we try to relate the three-dimensional concentration distribution $c(x,y,z,t)$ to the past and present values of c_0, q_0 and q_m.

As explained by Taylor (1953), the non-uniform velocity advects and rotates longitudinal gradients $\partial_x c_0$ to generate transverse gradients. In opposition to this, the combined effects of diffusion and boundary absorption are to erode the concentration variations towards the equilibrium profile $\psi_0(y,z)$. A representation which qualitatively reproduces this gradual advected process, and includes the fading influence of the discharge distribution across the flow, is

$$c = c_0(x,t)\,\psi_0(y,z) + \sum_{j=1}^{\infty}\int_0^{\infty} l_j(y,z,\tau)\,\partial_x^j c_0\Big(x-\int_0^{\tau} v_0(\tau')\,\mathrm{d}\tau',\, t-\tau\Big)\mathrm{d}\tau$$
$$+ \sum_{m=1}^{\infty}\sum_{j=0}^{\infty}\int_0^{\infty} f_{mj}(y,z,\tau)\,\partial_x^j q_m\Big(x-\int_0^{\tau} v_m(\tau')\,\mathrm{d}\tau',\, t-\tau\Big)\mathrm{d}\tau \tag{3.2}$$

(Smith 1982, equation (2.3)). Here l_j, f_{mj} are memory functions and $v_m(\tau)$ are memory displacement velocities. We remark that for a two-layer flow the series terminates after the first terms l_1, f_{10} (Thacker 1976).

Continuing as in De Gance & Johns (1978*a*, §3.2*c*), the one-dimensional equation governing the evolution of $c_0(x,t)$ is chosen to be the ψ_0 component of the full equations (2.1*a*, *b*). Using the representation (3.2) for $c(x,y,z,t)$, we obtain the integrodifferential equation

$$\partial_t c_0 + \lambda_0 c_0 + u_{00}\,\partial_x c_0 - \kappa_{00}\,\partial_x^2 c_0$$
$$+ \sum_{j=2}^{\infty}\int_0^{\infty}[\overline{ul_{j-1}\psi_0} - \overline{\kappa l_{j-2}\psi_0}]\,\partial_x^j c_0\Big(x-\int_0^{\tau} v_0(\tau')\,\mathrm{d}\tau',\, t-\tau\Big)\mathrm{d}\tau$$
$$= q_0 - \sum_{j=1}^{\infty}\sum_{m=1}^{\infty}[\overline{uf_{mj-1}\psi_0} - \overline{\kappa f_{mj-2}\psi_0}]\,\partial_x^j q_m\Big(x-\int_0^{\tau} v_m(\tau')\,\mathrm{d}\tau',\, t-\tau\Big)\mathrm{d}\tau. \tag{3.3}$$

It is the simple form of the c_0 and $\partial_x c_0$ coefficients that is the principal feature of this particular weighted average. By contrast, Sankarasubramanian & Gill (1973,

equation (8)) use a direct cross-sectional average and they have to contend with time-dependent coefficients for $c, \partial_x c$ as well as for the higher derivatives.

The lowest-order truncation of (3.3) which includes the effects both of velocity shear and of discharge non-uniformity is the delay-diffusion equation

$$\partial_t c_0 + \lambda_0 c_0 + u_{00}\partial_x c_0 - \kappa_{00}\partial_x^2 c_0 - \int_0^\infty \partial_\tau D\,\partial_x^2 c_0\Big(x - \int_0^\tau v_0(\tau')\,\mathrm{d}\tau', t-\tau\Big)\,\mathrm{d}\tau = q_0 - \sum_{m=1}^{\infty}\int_0^\infty \partial_\tau X_m\,\partial_x q_m\Big(x - \int_0^\tau v_m(\tau')\,\mathrm{d}\tau', t-\tau\Big)\,\mathrm{d}\tau, \tag{3.4}$$

with

$$\partial_\tau D = -\overline{ul_1\psi_0}, \quad \partial_\tau X_m = \overline{uf_{m0}\psi_0}. \tag{3.5}$$

Here D is the shear-dispersion coefficient and X_m is the centroid displacement associated with an mth-mode discharge. For a two-layer flow this truncated equation is exact. Except for the decay term $\lambda_0 c_0$, (3.4) is formally identical with that derived by the author (Smith 1982, equation (1.6)) for longitudinal dispersion with impermeable boundaries (see also Maron 1978). However, from the occurrence of the eigenmodes ψ_0, ψ_m in the definitions (2.4)–(2.6) and (3.5), we see that the coefficients $q_0, u_{00}, \kappa_{00}, \partial_\tau D, \partial_\tau X_m$ are all modified by the boundary absorption.

It is easy to confirm that, in accord with the work of Sankarasubramanian & Gill (1973), of De Gance & Johns (1978*a*), and of Lungu & Moffatt (1982), $c_0(x,t)$ eventually evolves as per the constant-coefficient diffusion equation

$$\partial_t c_0 + \lambda_0 c_0 + u_{00}\partial_x c_0 - [\kappa_{00} + D(\infty)]\partial_x^2 c_0 = q_0 - \sum_{m=1}^{\infty} X_m(\infty)\,\partial_x q_m. \tag{3.6}$$

To transfer the $\partial_x^2 c_0$ factor outside the integral in (3.4) it is necessary that the timescale for concentration variations greatly exceeds the memory timescale $1/\lambda_1$. A more stringent requirement is that the lengthscale greatly exceeds the displacement distance

$$\int_0^{1/\lambda_1} (v_0(\tau') - u_{00})\,\mathrm{d}\tau'.$$

At large times after discharge the lengthscale of the contaminant distribution grows as $t^{\frac{1}{2}}$. Thus the error in approximating the delay-diffusion equation (3.4) by the diffusion equation (3.6) decays as $t^{-\frac{1}{2}}$. This slowly decaying error is associated with the skewness (Chatwin 1970).

4. Evaluating the coefficients

To evaluate the coefficients $\partial_\tau D$, $\partial_\tau X_m$ and to optimize the choice for the displacement velocities $v_0(\tau)$, $v_m(\tau)$ we need to determine the functions l_1, f_{m0}, l_2, f_{m0}. Fortunately, the necessary analysis parallels that given previously by the author (Smith 1981, 1982).

The evolution equation (3.3) permits us to eliminate explicit t-derivatives in favour of x-derivatives. Thus, using the representation (3.2), all the terms in the full equations (2.1*a*, *b*) can be written as series of integrals of x-derivatives (Smith 1982, equation (3.4)). Equating successive coefficients of $\partial_x^j c_0$ and $\partial_x^j q_m$ to zero yields the equations satisfied by the memory functions l_j, f_{mj}:

$$\partial_\tau l_1 - \boldsymbol{\nabla}\cdot(\kappa\boldsymbol{\nabla} l_1) = 0, \tag{4.1a}$$

with

$$l_1 = (u_{00} - u)\,\psi_0 \quad \text{at} \quad \tau = 0, \tag{4.1b}$$

$$\kappa \boldsymbol{n}\cdot\boldsymbol{\nabla} l_1 + \beta l_1 = 0 \quad \text{on } \partial A; \tag{4.1c}$$

$$\partial_\tau f_{m0} - \boldsymbol{\nabla}\cdot(\kappa \boldsymbol{\nabla} f_{m0}) = 0, \tag{4.2a}$$

with

$$f_{m0} = \psi_m \quad \text{at} \quad \tau = 0, \tag{4.2b}$$

$$\kappa \boldsymbol{n}\cdot\boldsymbol{\nabla} f_{m0} + \beta f_{m0} = 0 \quad \text{on } \partial A; \tag{4.2c}$$

$$\partial_\tau l_2 - \boldsymbol{\nabla}\cdot(\kappa \boldsymbol{\nabla} l_2) = v_0(\tau)\, l_1 + (\overline{\psi_0 u l_1}\,\psi_0 - u l_1), \tag{4.3a}$$

with

$$l_2 = (\kappa - \kappa_{00})\,\psi_0 \quad \text{at} \quad \tau = 0, \tag{4.3b}$$

$$\kappa \boldsymbol{n}\cdot\boldsymbol{\nabla} l_2 + \beta l_2 = 0 \quad \text{on } \partial A; \tag{4.3c}$$

$$\partial_\tau f_{m1} - \boldsymbol{\nabla}\cdot(\kappa \boldsymbol{\nabla} f_{m1}) = v_m(\tau) f_{m0} + (\overline{\psi_0 u f_{m0}}\,\psi_0 - u f_{m0}), \tag{4.4a}$$

with

$$f_{m1} = 0 \quad \text{at} \quad \tau = 0, \tag{4.4b}$$

$$\kappa \mathbf{n}\cdot\boldsymbol{\nabla} f_{m1} + \beta f_{m1} = 0 \quad \text{on } \partial A. \tag{4.4c}$$

Equations (4.1)–(4.4) only differ from their counterparts in Smith (1981, 1982) by the presence of ψ_0. This change is exactly correct to compensate for the fact that the lowest mode is no longer constant. Hence the solutions for l_j, f_{mj} can be inferred directly from the solutions given by Smith (1981, equations (3.3), (4.2), (4.4); 1982, equations (4.3), (4.6)):

$$l_1 = -\sum_{m=1}^{\infty} u_{m0} \exp(-\lambda_m \tau)\,\psi_m(y,z), \tag{4.5}$$

$$f_{m0} = \exp(-\lambda_m \tau)\,\psi_m(y,z), \tag{4.6}$$

$$l_2 = \sum_{m=1}^{\infty} \left\{ \kappa_{m0} + u_{m0}\left[u_{mm}\tau - \int_0^\tau v_0(\tau')\,\mathrm{d}\tau' \right] + \sum_{\substack{n \neq m \\ n \neq 0}} u_{mn} u_{n0} \left[\frac{\exp(-\lambda_m \tau) - \exp(-\lambda_n \tau)}{\lambda_n - \lambda_m} \right] \right\} \psi_m(y,z), \tag{4.7}$$

$$f_{m1} = \left[\int_0^\tau v_m(\tau')\,\mathrm{d}\tau' - u_{mm}\tau \right] \psi_m(y,z) - \sum_{\substack{n \neq m \\ n \neq 0}} u_{mn} \left[\frac{\exp(-\lambda_m \tau) - \exp(-\lambda_n \tau)}{\lambda_n - \lambda_m} \right] \psi_n(y,z). \tag{4.8}$$

We can now evaluate the weighted averages (3.5) to obtain the results

$$\partial_\tau D = \sum_{m=1}^{\infty} u_{m0}^2 \exp(-\lambda_m \tau), \tag{4.9}$$

$$\partial_\tau X_m = u_{m0} \exp(-\lambda_m \tau). \tag{4.10}$$

Again we remark that in other weighted averages the counterparts to (4.9) and (4.10) are much less elegant. Indeed, Sankarasubramanian & Gill (1973) do not give explicit formulae for their time-dependent coefficients $K_1(t)$, $K_2(t)$. De Gance & Johns (1978*a*, §3.1 and table 1) give the formidable expressions from which K_1, K_2 can be computed.

The delay-diffusion equation (3.1) is equivalent to truncating the representation

(3.2) for $c(x,y,z,t)$ at the $\partial_x c_0$ and q_m terms. The truncation is at its most accurate when the inclusion of the subsequent $\partial_x^2 c_0$ and $\partial_x q_m$ terms make a minimal change to $c(x,y,z,t)$. From Smith (1982, equation (5.5)) we infer that this is achieved if

$$\overline{l_2(u-u_{00})\psi_0} = 0, \quad \overline{f_{m1}\psi_m} = 0. \tag{4.11a,b}$$

If we make the large-Péclet-number approximation

$$\kappa_{m0} \ll \frac{u_{m0}u_{mm}}{\lambda_m}, \tag{4.12}$$

then (4.11a,b) lead us to choose the memory velocities

$$\partial_\tau D\int_0^\tau v_0(\tau')\,\mathrm{d}\tau' = \tau\sum_{m=1}^{\infty} u_{mm}u_{m0}^2\exp(-\lambda_m\tau) + \sum_{m=1}^{\infty}\sum_{\substack{n\neq m\\ n\neq 0}} u_{m0}u_{n0}u_{mn}\left[\frac{\exp(-\lambda_m\tau)-\exp(-\lambda_n\tau)}{\lambda_n-\lambda_m}\right], \tag{4.13}$$

$$v_m(\tau) = u_{mm}. \tag{4.14}$$

We remark that shear dispersion is important precisely because most flows do have large Péclet numbers. Fife & Nicholes (1975) show that, in the opposite limit of small Péclet number, the diffusive limit (3.6) is achieved almost immediately (within a travel distance much less than the flow diameter) and the shear-dispersion coefficient $D(\infty)$ is much less than the diffusion term κ_{00}.

If the discharge conforms exactly to the ψ_0 mode (i.e. $q_m = 0$), then the constraint (4.11a) upon l_2 ensures that the first neglected term in (3.3) involves $\partial_x^4 c_0$. Taking moments of (3.3) we can readily infer that this term does not contribute to the area, centroid, variance or skewness. Thus all these moments are reproduced exactly by the model equation (3.4). For more general discharges the first neglected term involves $\partial_x^3 q_m$. Hence only the area, centroid and variance are exact. However, the dominant (growing) contribution to the third moment is associated with the left-hand-side terms. Therefore the skewness is asymptotically correct, and the dominant error is associated with the spikiness (kurtosis). This error decays at the rate t^{-1}.

A similar argument applies to the diffusion model derived by Sankarasubramanian & Gill (1973, equations (8), (11)), i.e. that the area, centroid and variance are exact. The advantages of the present approach (3.4)) are that the coefficients are simpler, the non-Gaussian character (i.e. persistent skewness) of the concentration distribution is revealed, and the linear superposition property is correctly reproduced (Smith 1982).

5. Boundary absorption in Poiseuille pipe flow

In a circular pipe of radius a and with constant molecular diffusivity κ the diffusion eigenmodes are Bessel functions

$$\psi_m = \frac{J_0(\gamma_m(r/a))}{[J_0(\gamma_m)^2+J_0'(\gamma_m)^2]^{\frac{1}{2}}}, \tag{5.1}$$

with

$$\lambda_m = \frac{\gamma_m^2\kappa}{a^2}, \quad \gamma_m J_0'(\gamma_m) + \frac{a\beta}{\kappa}J_0(\gamma_m) = 0, \tag{5.2}$$

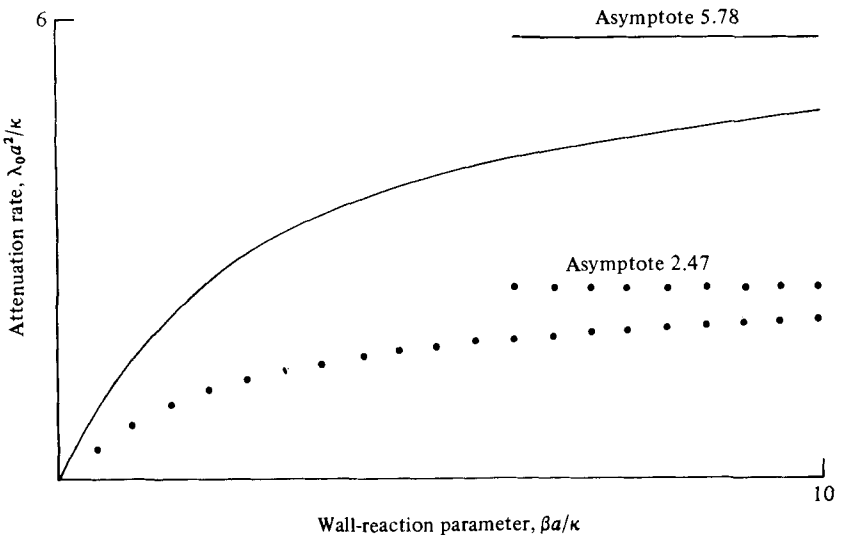

FIGURE 1. The attenuation rate λ_0 for pipe (——) and plane (· · · · · ·) Poiseuille flow as a function of the boundary absorption rate.

where J_0 is the zeroth-order Bessel function of the first kind. Figure 1 shows the attenuation rate λ_0 as a function of the wall-absorption parameter β (see also Sankarasubramanian & Gill 1973, figure 2; Lungu & Moffatt 1982, figure 1). As we might expect, λ_0 is a monotonic increasing function of β. Indeed, for small dimensionless reaction rate $B = a\beta/\kappa$ there is direct proportionality:

$$\lambda_0 \sim 2\kappa B, \quad \gamma_0^2 \sim 2B \quad \text{for} \quad B = \frac{a\beta}{\kappa} \ll 1. \tag{5.3}$$

However, for large $a\beta/\kappa$ the attenuation rate asymptotes to a constant. As explained by Sankarasubramanian & Gill (1973), it is the finite concentration gradient which limits the diffusive flux of contaminant towards the boundary. The main effect of the efficient removal of contaminant at the boundary is, therefore, to bring the concentration close to zero at the boundary.

For laminar flow with constant viscosity the velocity profile is parabolic:

$$u = 2\bar{u}\left[1 - \left(\frac{r}{a}\right)^2\right]. \tag{5.4}$$

Using the formulae (2.7a, b), or the integrals (4.8a, b) evaluated by Sankarasubramanian & Gill (1973, 1975), we find that the velocity coefficients (2.5) are given by

$$u_{mm} = \bar{u}\left\{1 + \frac{(\gamma_m^2 - 2B)^2 + \gamma_m^2 B^2}{3[\gamma_m^2 + B^2]\gamma_m^2}\right\}, \tag{5.5}$$

$$u_{mn} = -\frac{8\bar{u}\gamma_m\gamma_n[\gamma_m^2 + \gamma_n^2 + 2B^2]}{[\gamma_m^2 + B^2]^{\frac{1}{2}}[\gamma_n^2 + B^2]^{\frac{1}{2}}(\gamma_m^2 - \gamma_n^2)^2}. \tag{5.6}$$

Figure 2 shows the advection velocity u_{00} as a function of the wall-absorption parameter β (see also Sankarasubramanian & Gill 1973, figure 3; Lungu & Moffatt 1982, figure 1). We observe that u_{00} is an increasing function of β. Again the explanation of this fact was given by Sankarasubramanian & Gill (1973): the effect

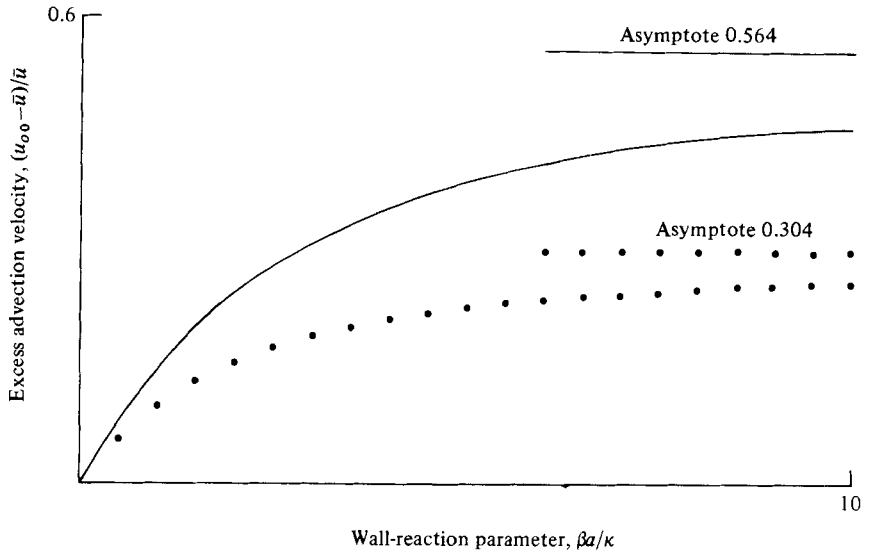

FIGURE 2. The advection velocity u_{00} for pipe (——) and plane (· · · · · ·) Poiseuille flow as a function of the boundary absorption rate.

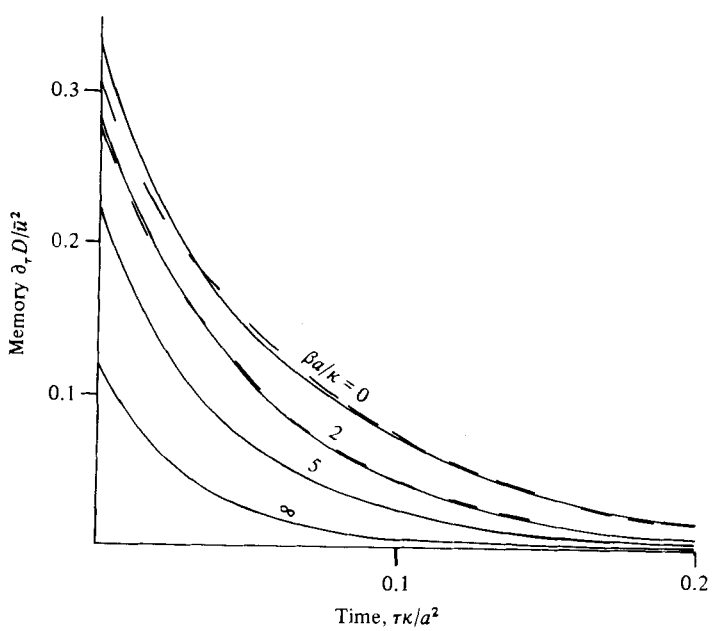

FIGURE 3. Exact (——) and telegraph-equation approximations (– – –) to the memory function $\partial_\tau D$ for Poiseuille pipe flow with boundary absorption.

of the wall reaction is to deplete solute in the slower-moving wall region, and therefore the solute distribution is weighed in favour of the faster-moving central region.

As β increases from zero to infinity, the boundary condition (2.2*b*) changes from zero flux to zero concentration, and the eigenfunctions ψ_m advance from m to $m+\frac{1}{2}$ oscillations. This more oscillatory character is associated with increased eigenvalues λ_m, and with decreased velocity coefficients u_{m0} (i.e., as β increases, the velocity

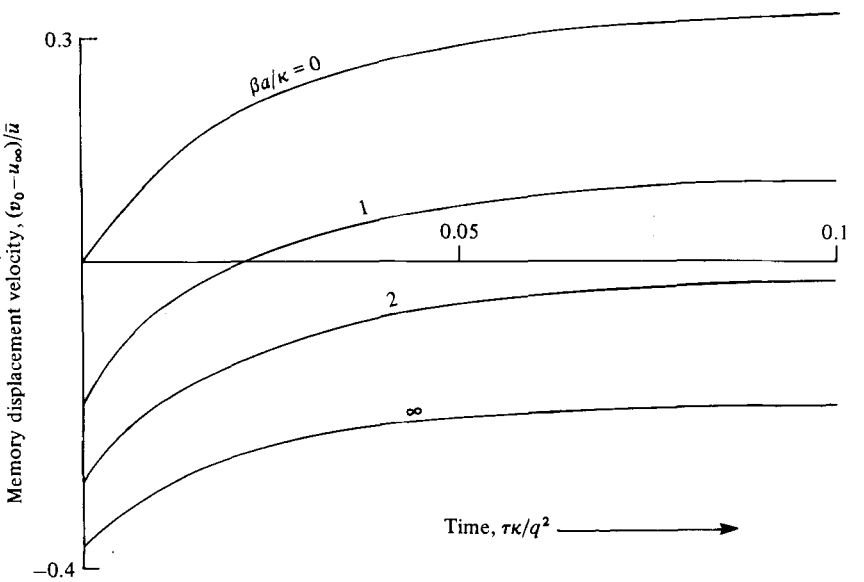

FIGURE 4. Velocity shift $v_0 - u_{00}$ for Poiseuille pipe flow, showing the tendency towards negative values when there is strong boundary absorption.

profile, with its zero value at the wall, more closely resembles the lowest mode ψ_0). Thus, from the formula (4.9) we infer that the wall absorption causes the memory function $\partial_\tau D$ to fade away more rapidly and to have a small magnitude than in the $\beta = 0$ case. These features are clearly apparent in figure 3. Yet again, a physical explanation for the reduced dispersion was given by Sankarasubramanian & Gill (1973): since velocity gradients are smaller in the central region of the tube than near the wall, and larger velocity gradients across the solute distribution cause larger axial dispersion, the result is a decrease in axial dispersion.

It deserves emphasis that, although the qualitative features are in accord with the work of Sankarasubramanian & Gill (1973), there are quantitative differences of order 20 % (De Gance & Johns 1978*b*, figures 1, 2, 4, 7). It is only at large times that the concentration profile across the flow settles down to the shape $\psi_0(y, z)$. Thus in the area-averaged results there are transient contributions from the higher modes ψ_m. These give rise to time dependence in the apparent attenuation rate and advection velocity, as well as to differences in the dispersion coefficient. Hence the mathematically preferred weighted-average results are simpler in character as well as in mathematical form.

The new feature of the delay-diffusion equation is that it goes on one stage further to encompass the third moment or skewness of the concentration distribution. The skewness is positive or negative according to whether the memory velocity $v_0(\tau)$ is greater or less than the advection velocity u_{00} (Smith 1981, equation (4.9)). Figure 4 shows that for Poiseuille pipe flow the effect of boundary absorption is to reduce or even to change the sign of the skewness. At small times we have the exact result

$$v_0(0) - u_{00} = \frac{\overline{(u-u_{00})^3 \psi_0^2}}{\overline{(u-u_{00})^2 \psi_0^2}}, \tag{5.7}$$

i.e. $v_0 - u_{00}$ is a weighted average of the shifted velocity profile $u(y, z) - u_{00}$. Since boundary absorption increases u_{00} (see figure 2), it follows from (5.7) that $v_0 - u_{00}$ tends

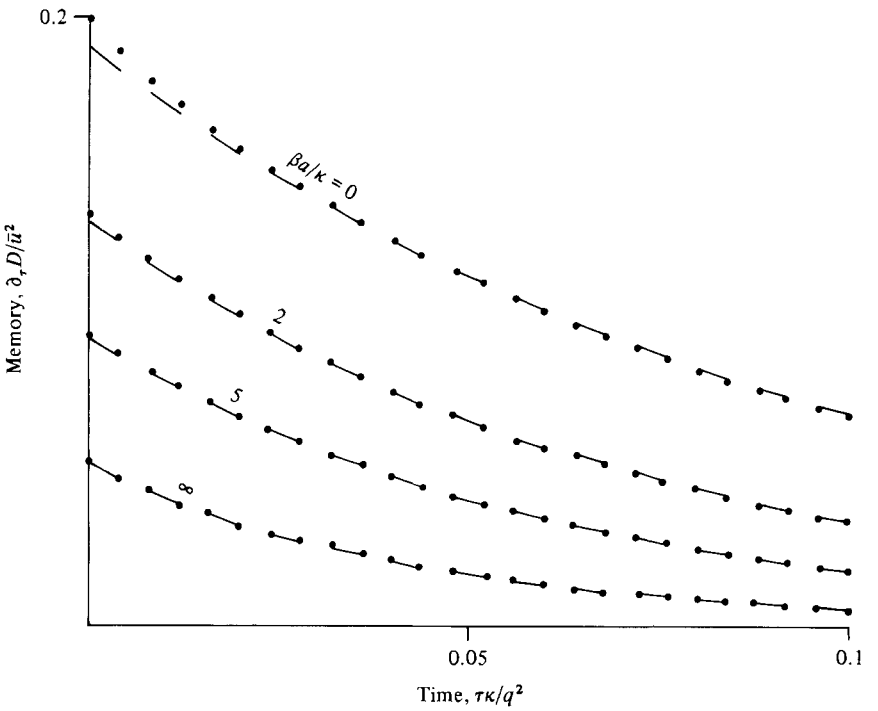

FIGURE 5. Exact (· · · · · ·) and telegraph-equation approximations (– – –) to the memory function $\partial_\tau D$ for plane Poiseuille flow with boundary absorption.

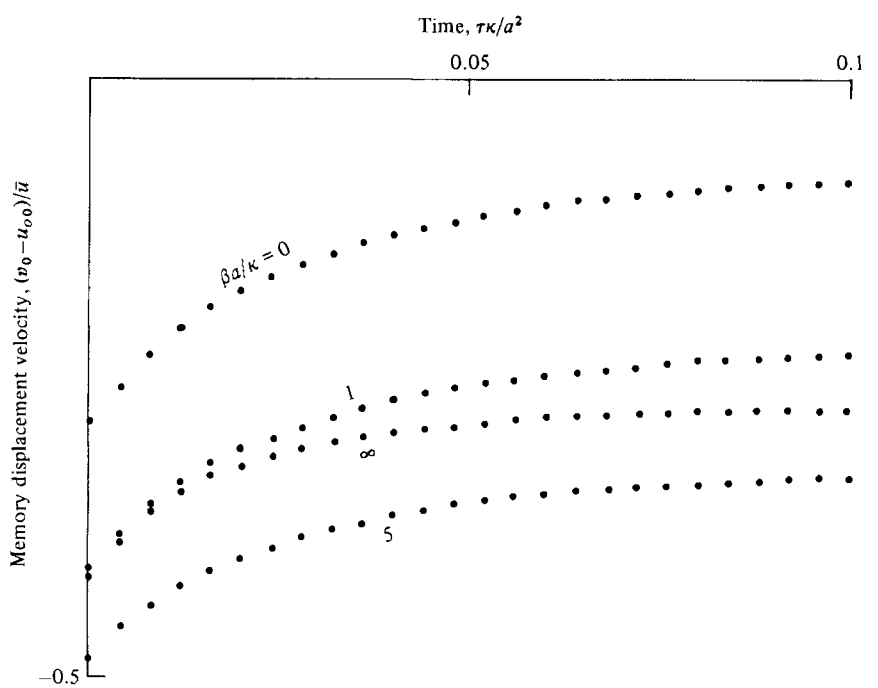

FIGURE 6. Velocity shift $v_0 - u_{00}$ for plane Poiseuille flow, showing the increased tendency for negative values when there is boundary absorption.

to be decreased. A physical explanation of this tendency towards negative skewness was given in the introduction (i.e. the small amount of slow-moving contaminant near the wall gets left behind as a trailing tail).

6. Plane Poiseuille flow

As a second illustrative example we follow Lungu & Moffatt (1982), and consider plane Poiseuille flow:

$$u(y) = \tfrac{3}{2}\bar{u}\left[1-\left(\frac{y}{a}\right)^2\right], \tag{6.1}$$

where $\bar{u}$ is the bulk velocity and $2a$ is the separation between the boundaries. The relevant eigenmodes and coefficients are

$$\psi_m = \cos\left(\frac{\gamma_m y}{a}\right)\left[\frac{2(\gamma_m^2+B^2)}{\gamma_m^2+B+B^2}\right]^{\frac{1}{2}}, \tag{6.2a}$$

with

$$\lambda_m = \frac{\gamma_m^2\kappa}{a}, \quad \gamma_m \tan\gamma_m = B = \frac{a\beta}{\kappa}, \tag{6.2b,c}$$

$$u_{mm} = \frac{\bar{u}}{\gamma_m^2+B+B^2}\left\{\gamma^2+B^2+\frac{3}{4\gamma_m^2}(B+B^2-\gamma_m^2)\right\}, \tag{6.2d}$$

$$u_{mn} = 6\bar{u}(-1)^{n+m+1}\frac{\gamma_n^2+\gamma_m^2+2B+2B^2}{(\gamma_n^2-\gamma_m^2)^2}\left[\frac{\gamma_n^2}{\gamma_n^2+B+B^2}\,\frac{\gamma_m^2}{\gamma_m^2+B+B^2}\right]^{\frac{1}{2}}. \tag{6.2e}$$

The dotted curves in figures 1 and 2 show the attenuation rate λ_0 and the advection velocity u_{00} as functions of the dimensionless absorption parameter $B = a\beta/\kappa$ (see also Lungu & Moffatt 1982, figure 1). The systematically lower results for λ_0 and u_{00} than in the pipe-flow case can be attributed to the fact that for the plane geometry there is only half as much boundary per unit cross-sectional area. For example, instead of the asymptote (5.3), we now have

$$\lambda_0 \sim \kappa B, \quad \gamma_0^2 \sim B \quad \text{for} \quad B = \frac{a\beta}{\kappa} \ll 1. \tag{6.3}$$

Figure 5 shows the memory function $\partial_\tau D$ for plane Poiseuille flow. The decay timescale is somewhat longer than in the pipe-flow case. However, the general features are in accord with figure 3 (i.e. more rapid decay and smaller magnitude as the wall absorption increases).

In the absence of boundary absorption the contaminant distribution in plane Poiseuille flow has negative skewness (Jayaraj & Subramanian 1978). Thus, even without boundary absorption the memory velocity $v_0(\tau)$ is less than the advection velocity u_{00} (Smith 1981, figure 6). Figure 6 confirms that this lagging behind becomes even more exaggerated when there is boundary absorption. We remark that for very large β there is so little contaminant close to the wall that there is a slight reversal in the trend towards increased skewness.

7. Telegraph equation

If we introduce the auxiliary function $g(y,z)$,

$$\nabla\cdot(\kappa\nabla g) = (u_{00}-u)\psi_0, \tag{7.1a}$$

with

$$\overline{g\psi_0} = 0, \quad \kappa\cdot\nabla g+\beta g = 0 \quad \text{on } \partial A, \tag{7.1b,c}$$

then we can derive the integral identities

$$D(\infty) = \overline{\psi_0 ug}, \quad \int_0^\infty [D(\infty) - D(\tau)]\,\mathrm{d}\tau = \overline{g^2}, \tag{7.2a,b}$$

$$\int_0^\infty \partial_\tau D \int_0^\tau v_0(\tau')\,\mathrm{d}\tau'\,\mathrm{d}\tau = \overline{ug^2}. \tag{7.2c}$$

Physically $g(y,z)$ is the perturbation from the asymptotic concentration profile $\psi_0(y,z)$ at large times after discharge.

Simple approximations to $\partial_\tau D$ and $v_0(\tau)$ which preserve the above identities are

$$\partial_\tau D = \mu D(\infty)\exp(-\mu\tau) \quad \text{with} \quad \mu = \frac{\overline{\psi_0 ug}}{\overline{g^2}}, \tag{7.3a,b}$$

$$v_0 = \frac{\overline{ug^2}}{\overline{g^2}} \tag{7.3c}$$

(Smith 1981, equations (5.4)–(5.9)). This can be thought of as being a one-mode approximation to the series (4.9)–(4.13), with the coefficients μ, $D(\infty)$, v_0 adjusted to achieve the best possible results at moderate to large times after discharge. Equivalently, the actual flow is approximated by two well-mixed layers with velocities (Smith 1981, equations (5.11))

$$u_\pm = \tfrac{1}{2}(u_{00}+v_0) \pm \{(\mu-\lambda_0)\,D(\infty) + \tfrac{1}{4}(v_0-u_{00})^2\}^{\frac{1}{2}}. \tag{7.4}$$

For the right-hand-side terms in the delay-diffusion equation (3.4), we note the identity

$$\int_0^\infty \partial_\tau X_m\,\mathrm{d}\tau = \frac{u_{m0}}{\lambda_m} = \overline{g\psi_m}. \tag{7.5}$$

Thus at moderately large times after discharge there is no need for us to know the individual modal contributions $q_m(x,t)$ to the discharge shape, and the summation on the right-hand-side of (3.4) can be replaced by the approximation

$$-\int_0^\infty \mu\exp(-\mu\tau)\,\partial_x[\overline{gq}(x-v_0\tau, t-\tau)]\,\mathrm{d}\tau. \tag{7.6}$$

The outcome of the above approximations (7.3) and (7.6) is that the delay-diffusion equation (3.4) can be transformed to a telegraph equation

$$(\partial_t + v_0\partial_x + \mu)(\partial_t + u_{00}\partial_x + \lambda_0 - \kappa_{00}\partial_x^2)\,c_0 - \mu D(\infty)\,\partial_x^2 c_0 = (\partial_t + v_0\partial_x + \mu)\,q_0 - \mu\,\partial_x(\overline{gq}), \tag{7.7}$$

(Smith 1982, equation (6.9)). By construction this equation inherits from the delay-diffusion equation (3.4) the properties that the area, centroid, variance and skewness are all asymptotically correct.

We remark that for a delta-function discharge, and with longitudinal diffusion negligible, the telegraph equation has an explicit solution. Thus, except for the attenuation factor $\exp(-\lambda_0 t)$, and the systematic replacement of μ by $\mu-\lambda_0$, the concentration profiles are precisely as illustrated in Smith (1981, figure 1; 1982, figure 3). At small times these profiles have the unrealistic feature of concentration spikes which move at the layer velocities u_+, u_-. However, these spikes decay exponentially fast on the memory timescale $1/(\mu-\lambda_0)$. In effect, this is the timescale on which modes other than $\psi_0(y,z)$ can be ignored, and knowledge of $c_0(x,t)$ alone gives a good indication of the full concentration distribution

$$c(x,y,z,t) \sim c_0(x,t)\,\psi_0(y,z) \quad \text{for} \quad (\mu-\lambda_0)\,t \gg 1. \tag{7.8}$$

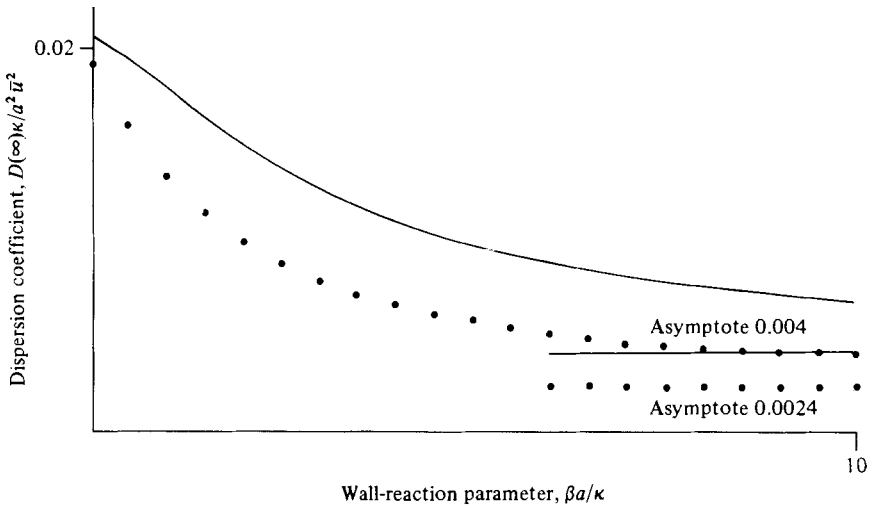

FIGURE 7. The long-term dispersion coefficient $D(\infty)$ for pipe (——) and plane (· · · · · ·) Poiseuille flow as a function of the boundary-absorption rate.

Even at times as large as $(\mu-\lambda_0)t = 15$, the telegraph equation solutions are noticeably skew. It is this very persistent skewness (Chatwin 1970) that permits the telegraph equation (5.7) to be accurate long before the diffusion equation (3.6), even though formally both model equations are large-time asymptotes.

8. Tests of the one-mode approximation

To apply the telegraph-equation analysis to pipe flow, we need to calculate both the lowest mode ψ_0 (see (5.1)), and the shape function g:

$$g = \left\{J_0\left(\frac{\gamma_0 r}{a}\right)\left[\frac{8}{\gamma_0^4}+\frac{2}{\gamma_0^2}-\frac{u_{00}}{\bar{u}\gamma_0^2}\right]-2\left(\frac{r}{a}\right)^2 J_0\left(\frac{\gamma_0 r}{a}\right)\frac{1}{\gamma_0^2}-\frac{8r}{a}J_0'\left(\frac{\gamma_0 r}{a}\right)\frac{1}{\gamma_0^3}\right.$$
$$\left.+\frac{8J_0'(\gamma_0)}{\gamma_0^3}+\frac{4J_0(\gamma_0)^2}{\gamma_0^3 J_0'(\gamma_0)}\right\}\frac{\bar{u}a^2}{\kappa[J_0(\gamma)^2+J_0'(\gamma_0)^2]^{\frac{1}{2}}}. \quad (8.1)$$

In principle, Schaftheitlin's reduction formula (Watson 1966, equation (5.14)) permits all the Bessel-function integrals $\overline{\psi_0 ug}$, $\overline{g^2}$, $\overline{ug^2}$ to be evaluated explicitly. This was done using an algebraic-manipulation computer program (CAMAL). Alas, the resulting expressions were found to be far too lengthy to be worthy of publication. The numerical results for $D(\infty)$, μ and v_0-u_{00} are shown in figures 7, 8 and 9 (see Sankarasubramanian & Gill 1973, figure 4). As noted in §5, wall absorption tends to reduce the longitudinal dispersion, reduce the memory timescale, and to change the sign of the skewness from positive to negative. The dashed curves in figure 3 reveal the accuracy of the one-mode approximation (7.3a) for $\partial_\tau D$. The error is imperceptible for the $B = 5$, $B = \infty$ curves.

For plane Poiseuille flow the shape function $g(y)$ takes the form

$$g = \frac{\bar{u}a^2}{\kappa}\left[\frac{2(\gamma_0^2+B^2)}{\gamma_0^2+B+B^2}\right]^{\frac{1}{2}}\left\{\cos\left(\frac{\gamma_0 y}{a}\right)\left[\frac{9}{\gamma_0^4}+\frac{3}{2\gamma_0^2}-\frac{u_{00}}{\bar{u}\gamma_0^2}\right]\right.$$
$$\left.+\frac{6y}{a}\sin\left(\frac{\gamma_0 y}{a}\right)\frac{1}{\gamma_0^3}-3\left(\frac{y}{a}\right)^2\cos\left(\frac{\gamma_0 y}{a}\right)\frac{1}{2\gamma_0^2}-\frac{3\gamma_0^2+6B+6B^2}{\gamma_0 B[\gamma_0^2+B^2]^{\frac{1}{2}}}\right\}. \quad (8.2)$$

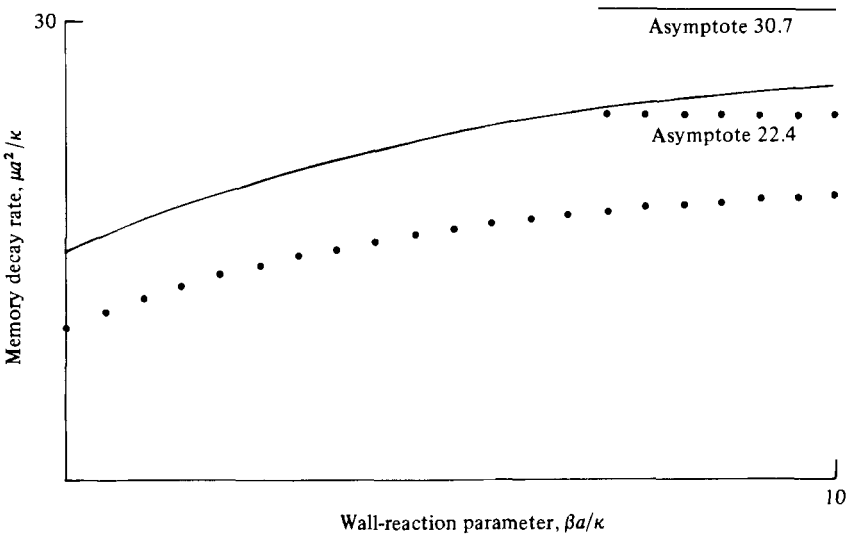

FIGURE 8. Memory decay rate μ for the telegraph-equation approximation to pipe (——) and plane (· · · · · · ·) Poiseuille flow when there is boundary absorption.

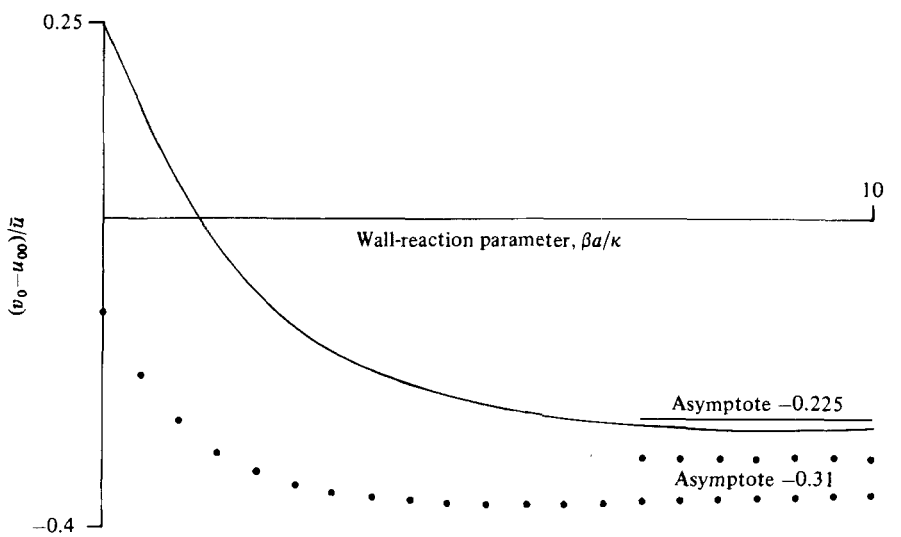

FIGURE 9. Velocity shift v_0-u_{00} for the telegraph-equation approximation to pipe (——) and plane (· · · · · ·) Poiseuille flow when there is boundary absorption.

Again, the explicit formulae for $\overline{\psi_0 ug}$, $\overline{g^2}$, $\overline{ug^2}$ are extremely lengthy (see Lungu & Moffatt 1982, equation (45)). The dotted curves in figures 7–9 show the numerical results for $D(\infty)$, μ and v_0-u_{00} (see Lungu & Moffatt 1982, figure 1). The dashed curves in figure 4 again show the high level of accuracy of the one-mode approximation for $\partial_\tau D$.

The ultimate test of either the delay-diffusion equation (3.4) or the telegraph equation (7.7) is to see how accurately they reproduce the actual concentration $c_0(x,t)$. To do this the full equation (2.1 a, b) were solved numerically for a uniform discharge

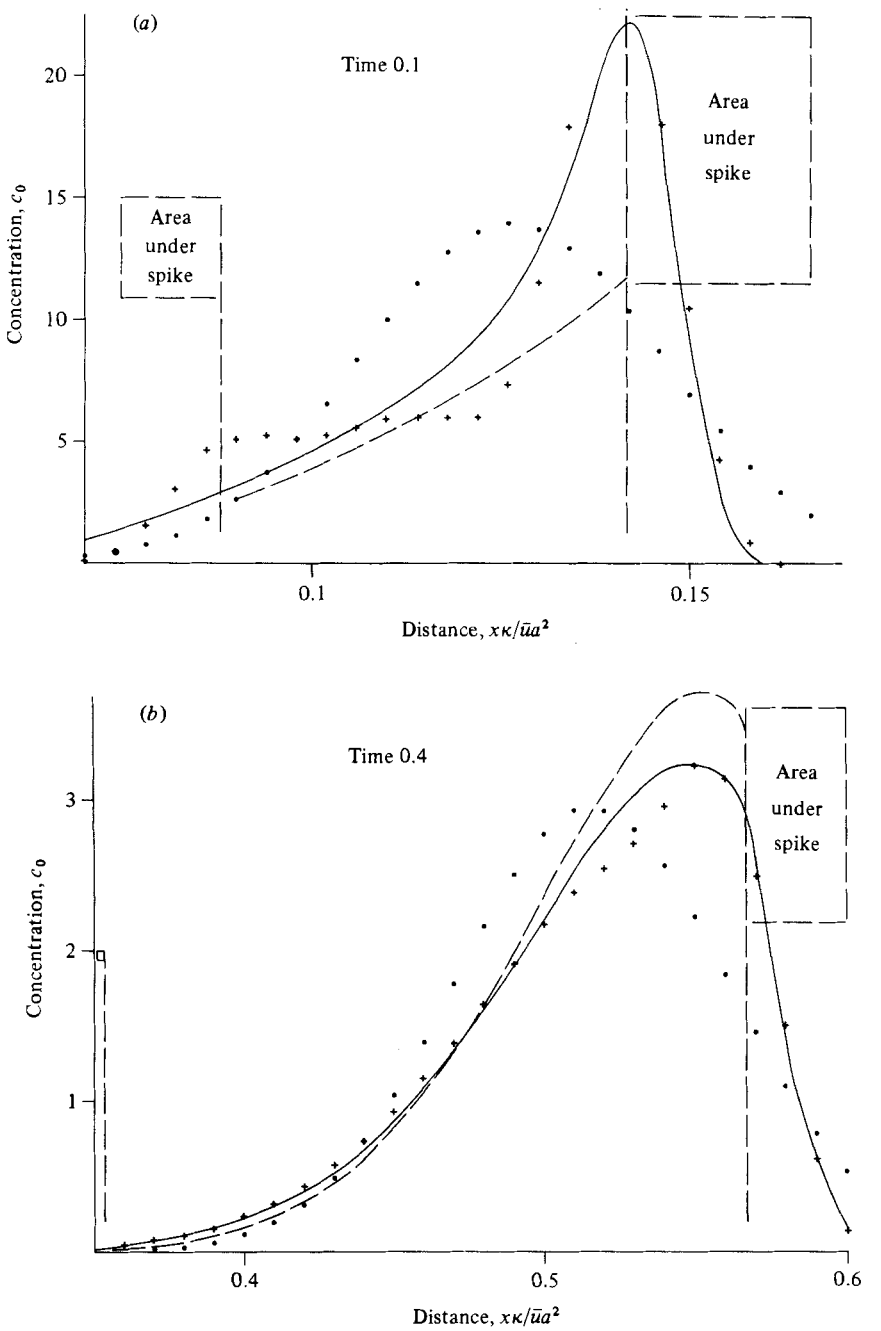

FIGURE 10. Exact (——), delay-diffusion (+ + +), Gaussian (· · · · · ·) and telegraph-equation (– – –) concentration profiles in plane Poiseuille flow.

in plane Poiseuille flow. The appropriate values of the coefficients q_m in the representation (2.4) of the source profile are

$$q_m = (-1)^m \frac{B}{\gamma_m}\left[\frac{2}{\gamma_m^2 + B + B^2}\right]^{\frac{1}{2}} \delta(x)\,\delta(t). \tag{8.3}$$

Figure 10 shows the exact, Gaussian, telegraph and delay-diffusion concentration profiles at the times

$$\frac{t\kappa}{a^2} = 0.1, 0.4 \quad \text{with} \quad B = 10^3, \quad \frac{\bar{u}a}{\kappa} = 5 \times 10^4, \quad \text{i.e.} \quad (\mu - \lambda_0)t \approx 2, 8. \tag{8.4}$$

A distinctive feature of the exact results is the skewness, very much more than in the case of zero boundary absorption (Jayaraj & Subramanian 1978, figures 3, 4; Smith 1982, figure 2; Smith 1981, figure 7). This persistent skewness is well represented by the delay-diffusion and telegraph-equation solutions. Which is, of course, what these model equations were designed to do.

9. Limits of applicability

Fischer *et al.* (1979, §5.5) have drawn attention to a contradiction inherent in the application of diffusion equation models for decaying substances. With minor modification their argument can be applied to boundary absorption. If the absorption is weak then it suffices that allowance is made for the slow exponential leakage of the contaminant. There is no need to calculate the advection velocity u_{00} and the longitudinal-dispersion coefficient $D(\infty)$ since the values can be taken to be those appropriate for impermeable boundary conditions. If instead the absorption is strong, then the contaminant concentrations decay rapidly on a timescale not very much longer than that for cross-sectional mixing (compare figures 1 and 8). However, the persistent skewness means that it takes many multiples of the timescale for cross-sectional mixing for the diffusion equation to become valid. Thus there are two possibilities: either the boundary absorption has negligible effect on the advection velocity u_{00} and on the shear dispersion coefficient $D(\infty)$, so the new calculations including boundary absorption are not necessary; or else nearly all the contaminant has been removed from the flow before the diffusion model has become applicable.

Fortunately, the full force of the above argument does not apply to the delay-diffusion or telegraph-equation models. Since the skewness is asymptotically correct, these model equations are applicable long before the diffusion model (3.6). It suffices that the concentration profile across the flow has settled down close to its asymptotic shape $\psi_0(y, z)$, and that any exaggerated (two-layer) spikiness no longer dominates the longitudinal concentration distribution. A reasonable criterion for both these requirements is

$$(\mu - \lambda_0)t > 4 \quad (\exp(-4) = 0.02), \tag{9.1}$$

i.e. intermediate between the cases shown in figures 10(*a*, *b*).

For heat in water with

$$\kappa = 1.4 \times 10^{-3} \text{ cm s}^{-1}, \quad a = 0.5 \text{ cm}, \quad \beta = \infty \tag{9.2}$$

the necessary lapse of time for pipe or plane Poiseuille flow respectively is

$$t > 28 \text{ s} \quad \text{or} \quad t > 36 \text{ s}. \tag{9.3}$$

In a household setting, the model equations are adequate to describe the transient behaviour in the pipework of a hot-water central-heating system, but not the more rapid temperature changes associated with the turning on of a hot-water tap.

In the very worst case, of pipe flow with $\beta = \infty$, $\frac{2}{5}$ of the contaminant remains in the flow by the time that the criterion (9.1) has been met. By contrast, the diffusion model of Sankarasubramanian & Gill (1973), as improved by De Gance & Johns

(1978*a*, *b*), requires four times as long as to achieve a comparable level of accuracy (i.e. with a skewness error of order $[(\mu-\lambda_0)t]^{-\frac{1}{2}}$ as compared with a kurtosis error of order $[(\mu-\lambda_0)t]^{-1}$). Thus there would only be about a fortieth of the contaminant left in the flow.

When the flow cross section does not conform to some analytically convenient form, the cross-sectional eigenvalue problem (2.2*a*, *b*) would need to be solved numerically. In such a case the one-dimensional delay-diffusion equation loses its computational advantage of the full advection–diffusion equations (2.1*a*, *b*). It is for such circumstances that the simpler telegraph equation model is pertinent. One possible example would be dispersion in rivers or estuaries with side pockets. In keeping with the above results (figures 10*a*, *b*), the retention of contaminant in side pockets is associated with marked skewness of the longitudinal concentration distribution (Nordin & Troutman 1980).

I wish to thank the referees for their constructive comments, and British Petroleum and the Royal Society for financial support.

REFERENCES

ARIS, R. 1959 On the dispersion of a solute by diffusion convection and exchange between phases. *Proc. R. Soc. Lond.* **A252**, 538–550.

CHATWIN, P. C. 1970 The approach to normality of the concentration distribution of a solute in solvent flowing along a straight pipe. *J. Fluid Mech.* **43**, 321–352.

DE GANCE, A. E. & JOHNS, L. E. 1978*a* The theory of dispersion of chemically active solutes in a rectilinear flow field. *Appl. Sci. Res.* **34**, 189–225.

DE GANCE, A. E. & JOHNS, L. E. 1978*b* On the dispersion coefficients for Poiseuille flow in a circular cylinder. *Appl. Sci. Res.* **34**, 227–258.

ELDER, J. W. 1959 The dispersion of marked fluid in turbulent shear flow. *J. Fluid Mech.* **5**, 544–560.

FIFE, P. C. & NICHOLES, K. R. K. 1975 Dispersion in flow through small tubes. *Proc. R. Soc. Lond.* **A344**, 131–145.

FISCHER, H. B., LIST, E. J., KOH, R. C. Y., IMBERGER, J. & BROOKS, N. H. 1979 *Mixing in Inland and Coastal Waters.* Academic.

GILL, W. N. & ANANTHAKRISHNAN, V. 1967 Laminar dispersion in capillaries: Part 4. The slug stimulus. *AIChE J.* **13**, 801–807.

JAYARAJ, K. & SUBRAMANIAN, R. S. 1978 On relaxation phenomena in field-flow fractionation. *Sep. Sci. Tech.* **13**, 791–817.

LUNGU, E. M. & MOFFATT, H. K. 1982 The effect of wall conductance on heat diffusion in duct flow. *J. Engng Math.* **16**, 121–136.

MARON, V. I. 1978 Longitudinal diffusion through a tube. *Intl J. Multiphase Flow* **4**, 339–355.

NORDIN, C. F. & TROUTMAN, B. M. 1980 Longitudinal dispersion in rivers: the persistence of skewness in observed data. *Water Resources Res.* **16**, 123–128.

SANKARASUBRAMANIAN, R. & GILL, W. N. 1973 Unsteady convective diffusion with interphase mass transfer. *Proc. R. Soc. Lond.* **A333**, 115–132.

SANKARASUBRAMANIAN, R. & GILL, W. N. 1975 Correction to: 'Unsteady convective diffusion with interphase mass transport'. *Proc. R. Soc. Lond.* **A341**, 407–408.

SMITH, R. 1981 A delay-diffusion description for contaminant dispersion. *J. Fluid Mech.* **105**, 469–486.

SMITH, R. 1982 Non-uniform discharges of contaminants in shear flows. *J. Fluid Mech.* **120**, 71–89.

TAYLOR, G. I. 1953 Dispersion of soluble matter in solvent flowing slowly through a tube. *Proc. R. Soc. Lond.* **A219**, 186–203.

THACKER, W. C. 1976 A solvable model of shear dispersion. *J. Phys. Oceanogr.* **6**, 66–75.

WATSON, G. N. 1966 *A Treatise on the Theory of Bessel Functions.* Cambridge University Press.